the microscopic structure of the adsorbed O_2 has changed. The lack of diffraction peaks indicates that this is a liquid-glass, rather than a liquid-crystalline solid transition such as occurs in larger pores.

The scattering measurements indicate that an amorphous solid phase is formed in the small pores at low temperature. The structure of this solid phase is quite unusual. The local ordering in the solid, as reflected by the variations in $S(Q)$, is much less than that in the liquid phase. This is quite different from other amorphous systems, such as glasses, where the local ordering is similar to that of the liquid and the structure in $S(Q)$ usually sharpens slightly with respect to the liquid when the glass forms, reflecting the increased atomic correlations in the glass phase (*19*). However, our results indicate that the atomic correlations of the solid phase in the pores are significantly smaller than those of the liquid. In fact, the almost complete disappearance of structure in $S(Q)$ upon cooling indicates that correlations between atoms in the solid are extremely small. Such a transition where the solid exhibits much less order than the liquid is, to our knowledge, unique.

It is important to emphasize that the decrease in structure of $S(Q)$ upon cooling is not caused by the migration of material out of the pore space. The total scattering at large Q, which is proportional to the amount of material in the pores, does not change significantly upon cooling. Thus, the oxygen in the pores does not migrate to other regions out of the neutron beam, and our results are representative of the freezing of oxygen in these small pores.

The origin of this solid phase is not clear at present. It must, however, be related to the large surface to volume ratio in the small-pore samples. Each oxygen molecule adsorbed in the pores feels a significant interaction with the walls because of the strong substrate-adsorbate interaction. This leads to a frustration in which the oxygen molecules cannot minimize energy with respect to both neighboring molecules and the surrounding random porous medium at the same time. Thus, the solid phase that is formed is a compromise between these competing influences and exhibits almost no correlations between the oxygen molecules in the pores.

A simple physical interpretation emerges from these results. Near the walls, the molecules are strongly influenced by the complex amorphous structure of the walls. They accommodate this structure as best they can, leading to an added amorphous component in the scattering observed for the large-pore samples. There is then a healing length away from the walls where the disorder induced by the walls is annealed out. For large pores, this annealing process is complete, and a crystalline phase appears in the center of the pores. For smaller pores, the disorder cannot anneal out, and a unique glass phase is formed.

REFERENCES AND NOTES

1. J. Klafter and J. M. Drake, *Molecular Dynamics in Restricted Geometries* (Wiley, New York, 1989).
2. J. Warnock, D. D. Awschalom, M. W. Shafer, *Phys. Rev. Lett.* **57**, 1753 (1986).
3. C. L. Jackson and G. B. McKenna, *Rubber Chem. Technol.* **64**, 760 (1990).
4. R. H. Torii, H. J. Maris, G. M. Seidel, *Phys. Rev. B* **41**, 7167 (1990).
5. E. Molz, A. P. Y. Wong, M. H. W. Chan, *ibid.* **48**, 5741 (1993).
6. M. B. Ritter, D. D. Awschalom, M. W. Shafer, *Phys. Rev. Lett.* **61**, 966 (1988).
7. W.-J. Ma, J. R. Banavar, J. Koplik, *J. Chem. Phys.* **97**, 485 (1992).
8. P. E. Sokol *et al.*, *Appl. Phys. Lett.* **61**, 777 (1992).
9. R. K. Iler, *The Chemistry of Silica* (Wiley, New York, 1979).
10. J. W. Stewart, *J. Phys. Chem. Solids* **12**, 122 (1959).
11. M. F. Collins, *Proc. Phys. Soc. London* **89**, 415 (1966).
12. R. J. Meier, R. B. Helmholdt, *Phys. Rev. B* **29**, 1387 (1984).
13. T. H. Jordan, W. E. Streib, H. Warren, *Acta Crystallogr.* **17**, 777 (1964).
14. D. D. Awschalom, J. Warnock, M. W. Schafer, *Phys. Rev. Lett.* **57**, 1607 (1986).
15. P. A. Egelstaff, in *Methods of Experimental Physics*, D. L. Price and K. Skold, Eds. (Academic Press, New York, 1987), vol. 23, part B, pp. 405–468.
16. K. S. Pederson, F. Y. Hansen, K. Carneiro, *J. Chem. Phys.* **70**, 1051 (1979).
17. W. Schmatz, in (*15*), pp. 85–126.
18. H. P. Klug and H. P. Alexander, *X-ray Diffraction Procedures for Polycrystalline and Amorphous Materials* (Wiley, New York, 1974).
19. S. Kenji, in (*15*), pp. 243–300.

20. This work was supported by National Science Foundation grant DMR-91-23469, Petroleum Research Fund contract 26046-AC7E, Gas Research Institute contract 50872601473, and Office of Basic Energy Science–Division of Materials Research support of the Intense Pulsed Neutron Source at Argonne National Laboratory under Department of Energy grant W-31-109-ENG-38. B.S.S. acknowledges the support of the Division of Educational Programs at Argonne National Laboratory.

5 May 1994; accepted 11 October 1994

Host Range of a Plant Pathogenic Fungus Determined by a Saponin Detoxifying Enzyme

P. Bowyer, B. R. Clarke, P. Lunness, M. J. Daniels, A. E. Osbourn*

Antifungal saponins occur in many plant species and may provide a preformed chemical barrier to attack by phytopathogenic fungi. Some fungal pathogens can enzymatically detoxify host plant saponins, which suggests that saponin detoxification may determine the host range of these fungi. A gene encoding a saponin detoxifying enzyme was cloned from the cereal-infecting fungus *Gaeumannomyces graminis*. Fungal mutants generated by targeted gene disruption were no longer able to infect the saponin-containing host oats but retained full pathogenicity to wheat (which does not contain saponins). Thus, the ability of a phytopathogenic fungus to detoxify a plant saponin can determine its host range.

Plant disease resistance may be mediated by active responses, triggered after pathogen attack, and by preformed substances that serve as plant protectants. Saponins (glycosylated steroidal or triterpenoid compounds) are common plant secondary metabolites occurring in over 100 families, and because many saponins have pronounced antifungal properties, it is possible that they act as preformed determinants of resistance to attack by fungi (*1–4*). The toxic effects of saponins are attributed to their ability to form complexes with membrane sterols, resulting in loss of membrane integrity (*5, 6*). Some pathogenic fungi have intrinsic resistance to the membraneolytic action of saponins because of their membrane composition (*4, 7*), whereas others produce enzymes that specifically detoxify particular plant saponins (*4, 8–14*). These enzyme activities have been associated with the ability to attack certain plants. This implies that, at least for some interactions, "saponin-saponinase" combinations may dictate the outcome of attempted infection of plants by fungi.

A paradigm case is the interaction between the root-infecting fungus *Gaeumannomyces graminis* and cereals. Isolates of G. *graminis* that infect oats (G. *graminis* var. *avenae*, or Gga) are relatively insensitive to the oat root saponin avenacin A-1, whereas G. *graminis* var. *tritici* (Ggt) isolates are unable to infect most oat species and are sensitive to avenacin A-1 (*8–10*). Both Gga and Ggt are pathogenic to the non–saponin-containing host, wheat. Avenacin A-1 is localized in the epidermal cells of the oat root (*15*) and hence may constitute one of the first barriers to infection by sensitive fungi such as Ggt. The one oat species that lacks avenacin A-1, *Avena longiglumis*, is susceptible to infection by Ggt (*15*). These observations are consistent with a role for avenacin A-1 as a determinant of resistance

The Sainsbury Laboratory, John Innes Centre, Norwich Research Park, Norwich NR4 7UH, UK.

*To whom correspondence should be addressed.

to fungal attack. The insensitivity of the oat-attacking (*Gga*) variety of G. *graminis* to avenacin A-1 has been attributed to the ability of *Gga* isolates to produce the saponin-detoxifying enzyme avenacinase (*8*). Here we describe the cloning of the gene encoding avenacinase and demonstrate that targeted disruption of this gene produces saponin-sensitive fungal mutants with a reduced host range.

The *Gga* extracellular enzyme avenacinase can remove both the β-1,2– and the β-1,4–linked terminal D-glucose molecules from the oat root saponin avenacin A-1 to give first the mono- and then the bis-deglucosylated form, both of which are substantially less toxic to fungi than is avenacin A-1 itself (*8*, *9*). A single purified protein is able to catalyze both hydrolytic steps required for avenacinase action (*10*).

The gene for avenacinase was cloned by a reverse genetics approach (*16*). Avenacinase was purified from culture filtrates of *Gga*. Polyclonal antisera to avenacinase were raised in rats and used to select immunoreactive phage plaques from a lambda gt11 complementary DNA (cDNA) expression library derived from *Gga* mRNA. Eight cDNA clones were isolated and found to cross-hybridize and to contain common restriction fragments, which indicated that the clones were related. A genomic DNA clone containing the putative avenacinase gene (*pA3G1*) was isolated by homology to the cDNA clone *pA312* (*16*). When this genomic DNA clone and the total genomic DNA of *Gga* were digested with a number of restriction enzymes and hybridized with pA312, a single copy of the avenacinase gene was detected in the *Gga* genome. Northern (RNA) blot analysis of RNA from a number of *Gga* isolates revealed a single RNA band of approximately 3 kb that hybridized with pA312 [which is consistent with the size of the avenacinase protein (110 kD)].

The genomic clone pA3G1 was tested for its ability to encode avenacinase by expression in the heterologous fungus *Neurospora crassa*, which is avenacin A-1–sensitive and has no detectable avenacinase activity. This was achieved by cotransformation of an auxotrophic (*pyr4*) mutant of *N. crassa* with pA3G1 and with the plasmid pGM32 (containing the *pyr4*$^+$ gene, which restores the *pyr4* mutant to prototrophy) (*17*, *18*). Transformants were first selected for a *pyr4*$^+$ phenotype and then tested for increased resistance to avenacin A-1 (10 μg/ml). A proportion of the *pyr4*$^+$ transformants that had received pGM32 were also expected to contain the plasmid pA3G1, bearing the cloned *Gga* DNA. Four out of 30 *pyr4*$^+$ transformants tested showed increased resistance to avenacin A-1. Only these four transformants contained pA3G1 DNA and had avenaci-

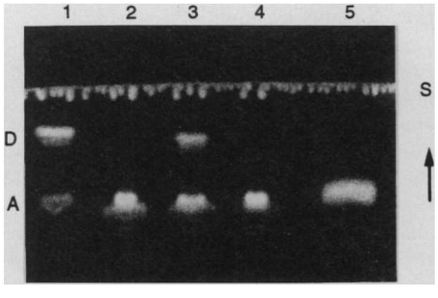

Fig. 1. Heterologous expression of the cloned avenacinase gene from *Gga* in *N. crassa*. Avenacinase activity of culture filtrates of fungi assayed by thin-layer chromatography (*10*). A and D represent the positions of avenacin A-1 and of its mono-deglucosylated product, respectively. S, solvent front. Lane 1, *Gga* (isolate A3); lane 2, *Ggt* (isolate T5); lane 3, *N. crassa* transformed with the avenacinase genomic clone pA3G1; lane 4, untransformed *N. crassa*; and lane 5, avenacin A-1 standard.

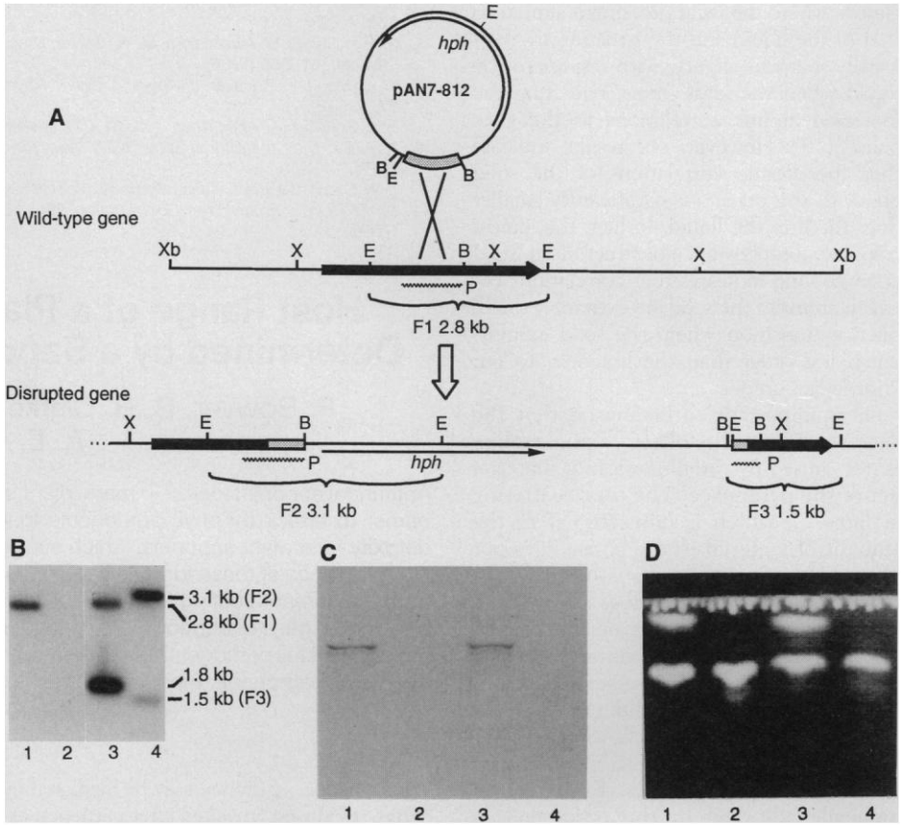

Fig. 2. Targeted disruption of the avenacinase gene. (**A**) Plasmid pAN7-812 was derived by cloning of an internal segment (stippled area) of the avenacinase gene into a modified pAN7-1 vector (which carries *hph*, a gene encoding resistance to hygromycin B) (*21*). Cleavage sites for the restriction enzymes Xba I (Xb), Xho I (X), Bam HI (B), and Eco RI (E) are indicated. pAN7-812 was transformed into *Gga* (isolate A3) with selection for hygromycin resistance according to standard procedures (*22*). Integration by homologous recombination of the plasmid into the avenacinase coding region (solid arrow) gives insertional inactivation of the avenacinase gene. Of 100 hygromycin-resistant transformants, 5 were avenacin A-1–sensitive. Five hygromycin-resistant transformants that retained wild-type avenacin A-1 resistance and did not have a disrupted avenacinase gene were included as controls in subsequent experiments. Typical examples from these experiments are shown in (B) through (D), in which lane 1 shows wild-type *Gga* (isolate A3), lane 2 shows wild-type *Ggt* (isolate T5), lane 3 shows a *Gga* transformant that has not undergone disruption of the avenacinase gene and displays wild-type resistance to avenacin A-1 (A3 T-10), and lane 4 shows an avenacinase-minus *Gga* transformant (A3 T-1) generated by gene disruption. (**B**) Southern blot of Eco RI–digested genomic DNA [10 μg per lane, prepared by standard techniques (*23*)] probed with a fragment of the avenacinase gene [shown as a bar P in (A)]. The predicted Eco RI fragments (F1, F2, and F3) are marked in (A) for the intact avenacinase gene (F1, 2.8 kb) and for the gene disruption (F2, 3.1 kb, and F3, 1.5 kb). Lane 1 shows the predicted wild-type *Gga* band; lane 2 (*Ggt*) shows no hybridizing band; lane 3 (A3 T-10) shows a wild-type 2.8-kb band characteristic of an intact avenacinase gene, together with a 1.8-kb band probably resulting from integration of pAN7-812 elsewhere in the genome; and lane 4 (A3 T-1) shows a pattern consistent with homologous integration. (**C**) Protein immunoblot of fungal culture filtrates developed with antiavenacinase antisera. A signal can clearly be seen in wild-type *Gga* and in A3 T-10 (lanes 1 and 3) but not in *Ggt* (lane 2) or in A3 T-1 (lane 4). (**D**) Avenacinase activity (*10*) can be detected in culture filtrates of wild-type *Gga* (lane 1) and in A3 T-10 (lane 3) but not in *Ggt* or A3 T-1 (lanes 2 and 4).

nase activity (Fig. 1). Protein immunoblot analysis with antiavenacinase antisera showed that the avenacin A-1–resistant transformants all produced a cross-reacting protein of the same size as the native avenacinase from *Gga*. This protein was not produced by untransformed *N. crassa* or by transformants that had received pGM32 but not pA3G1.

Avenacinase-minus mutants of *Gga* were obtained by transformation-mediated targeted disruption of the avenacinase gene (Fig. 2A) (*19*). Transformants were screened for resistance to avenacin A-1, and a number of avenacin A-1–sensitive transformants were identified. This sensitivity to avenacin A-1 correlated with the disruption of the avenacinase gene as assessed by Southern (DNA) blot analysis. Transformants in which plasmid DNA had integrated into the avenacinase gene (Fig. 2B) were eight to nine times more sensitive to avenacin A-1, no longer produced a protein that cross-reacted with the antiavenacinase antisera (Fig. 2C), and had no detectable avenacinase activity (Fig. 2D). Transformed fungi with an intact avenacinase gene (due to ectopic integration of the transforming plasmid) showed wild-type degrees of avenacin resistance, retained the immunologically cross-reactive protein, and had wild-type amounts of avenacinase activity (Fig. 2, B through D). A separate disruption experiment with a 3′ internal fragment of the avenacinase gene generated a mutant that produced a truncated protein [approximately 90 kD instead of the wild-type value of 110 kD (*10*)] with 20 to 25% of wild-type avenacinase specific activity. The experiments involving heterologous expression and generation of null mutants and of mutants producing a truncated avenacinase protein all indicated that the cloned DNA contains the avenacinase structural gene.

Targeted disruption of the avenacinase gene rendered *Gga* unable to cause disease on oats but had no discernible effect on its pathogenicity to wheat (Fig. 3). Microscopic examination of inoculated seedlings indicated that the mutant fungus could no longer penetrate oat roots. Avenacin A-1 detoxification is therefore an absolute requirement for pathogenicity of *Gga* to oats. Interestingly, the mutant that produced a truncated, less active enzyme also gave almost no symptoms on oats (pathogenicity score = 1.7 ± 0.6; see legend to Fig. 3). This may imply that a threshold amount of avenacinase is required for pathogenicity to oats. Because avenacinase-deficient mutants are still fully pathogenic to wheat, the fundamental ability of the fungus to infect and to cause disease does not require the enzyme. Therefore, avenacinase can be viewed as a determinant of host range.

The wide distribution of saponins in plants (*1*, *4*), together with the occurrence of specific saponin-degrading enzymes in diverse phytopathogenic fungi (*4*, *8*–*14*), suggest a general role for saponin detoxification in the infection of plants by fungi. Saponin-saponinase combinations may therefore be more important in determining host range than has hitherto been appreciated. In future, crop protection strategies involving inhibitors of saponinases or manipulation of saponin biosynthetic pathways may complement approaches that exploit the plant's resistance mechanisms that are induced after infection (*20*).

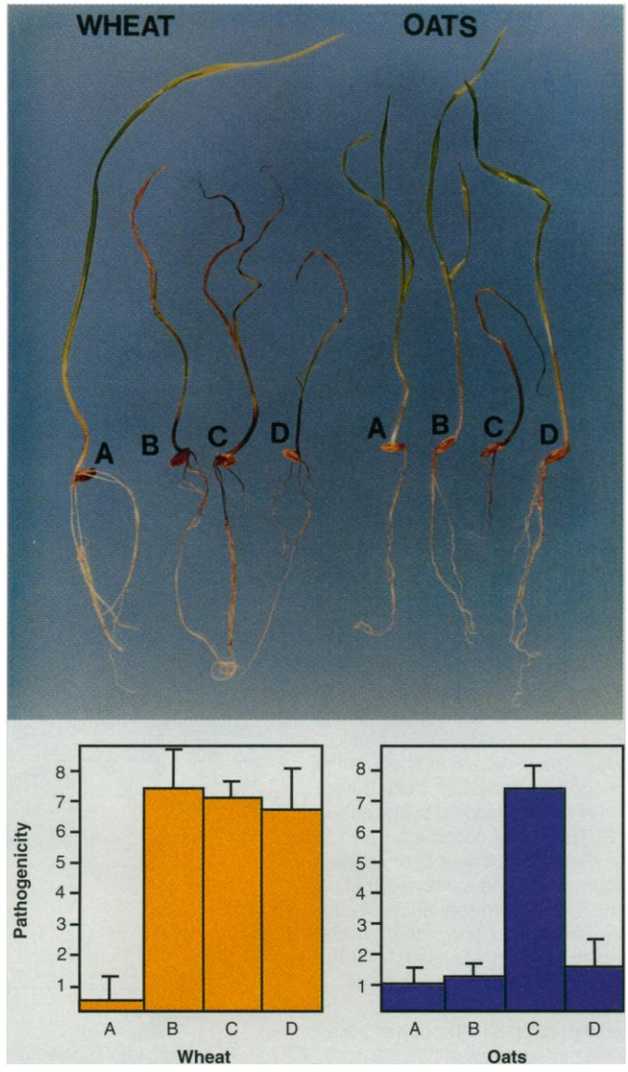

Fig. 3. Pathogenicity of wild-type and mutant fungi to wheat and oats. Treatments are: (**A**) mock inoculation, (**B**) wild-type *Ggt* (isolate T5), (**C**) wild-type *Gga* (isolate A3), and (**D**) A3 T-1 (avenacinase-minus mutant of the *Gga* isolate A3). The upper panel shows the appearance of the seedlings, whereas the lower panel gives mean pathogenicity scores (50 seedlings per treatment; error bars represent 95% confidence limits) (*24*). Pathogenicity was scored on an arbitrary scale of 0 to 8; 0, no disease symptoms; 1, some browning of the roots, which may be nonspecific; 2, a single lesion visible on the roots; 3, several lesions visible; 4, as 3, but one lesion confluent with seed; 5, as 3, but more than one lesion confluent with seed; 6, extensive root necrosis and browning of the leaf sheath; 7, as 6 and leaves wilting and chlorotic; 8, as 6, and leaves brown and necrotic. The wild-type *Gga* was pathogenic to oats, causing severe root lesions and blackening of the crown, whereas the avenacinase-minus *Gga* mutant A3 T-1 produced no discernible disease symptoms on this host. *Ggt*, *Gga*, and A3 T-1 were all strongly pathogenic to wheat. *Gga* transformants such as A3 T-10, which contain an intact avenacinase gene, produced symptoms indistinguishable from those produced by wild-type *Gga* on both oats and wheat (*25*).

REFERENCES AND NOTES

1. K. R. Price, I. T. Johnson, G. R. Fenwick, *CRC Crit. Rev. Food Sci. Nutr.* **26**, 27 (1991).
2. S. B. Mahato, S. Sarkar, G. Poddar, *Phytochemistry* **28**, 3037 (1988).
3. S. B. Mahato and A. K. Nando, *ibid.* **30**, 1357 (1991).
4. F. Schönbeck and E. Schlösser, in *Physiological Plant Pathology*, R. Heitefuss and P. H. Williams, Eds. (Springer-Verlag, Berlin, 1976), pp. 653–678.
5. A. D. Bangham and R. W. Horne, *Nature* **196**, 952 (1962).
6. R. R. Dourmaskin, R. M. Dougherty, R. J. C. Harris, *ibid.* **194**, 1116 (1962).
7. P. A. Arneson and R. D. Durbin, *Phytopathology* **58**, 536 (1968).
8. E. M. Turner, *J. Exp. Bot.* **12**, 169 (1961).
9. W. M. L. Crombie, L. Crombie, J. B. Green, J. A. Lucas, *Phytochemistry* **25**, 2075 (1986).
10. A. E. Osbourn, B. R. Clarke, J. Dow, M. Daniels, *Physiol. Mol. Plant Pathol.* **38**, 301 (1991).
11. R. D. Durbin and J. F. Uchytil, *Biochim. Biophys. Acta* **191**, 176 (1969).
12. G. F. Pegg and G. F. Woodward, *Physiol. Mol. Plant Pathol.* **28**, 187 (1986).
13. J. E. Ford, D. J. McCance, R. B. Drysdale, *Phytochemistry* **16**, 545 (1977).
14. K. Verhoeff and J. I. Liem, *Phytopathol. Z.* **82**, 333 (1975).
15. A. E. Osbourn, B. R. Clarke, P. Lunness, P. R. Scott, M. J. Daniels, *Physiol. Mol. Plant Pathol.* **45**, 457 (1994).
16. Avenacinase was prepared from culture filtrate of the *Gga* isolate A3 by ammonium sulfate precipitation, isoelectric focusing (IEF), and high-performance liquid chromatography (HPLC) gel filtration. Proteins were precipitated by addition of ammonium sulfate to 80%

saturation. After resuspension and dialysis [20 mM tris-HCl (pH 7.5)], the proteins were separated by IEF in the pH range 4 to 6.5 with the RF3 Protein Fractionator (Texas Instruments). Active fractions were pooled, desalted, and exchanged into 20 mM sodium phosphate buffer (pH 7.0) with 0.2 M sodium chloride with the use of Centricon C-30 spin columns (Amicom, Beverly, MA). Gel filtration was done on a 7.8 × 250 mm TSK G3000 SW XL HPLC column (Tosoh Corporation, Japan) in the same buffer. Active fractions were pooled and then fractionated by SDS–polyacrylamide gel electrophoresis. The band corresponding to avenacinase (*10*) was electroeluted and used to immunize Wistar rats. The resulting polyclonal antiserum was used for protein immunoblot analysis and cDNA library screening at a dilution of 1:2000. Control experiments with preimmune serum (diluted 1:100) gave no signal. Rabbit antibody to rat immunoglobulin G alkaline phosphatase conjugate was used as the secondary antibody. A *Gga* cDNA expression library was constructed in lambda gt11 by standard methods [J. M. Chirgwin, A. E. Przybyla, R. J. MacDonald, W. Rutter, *Biochemistry* **18**, 5294 (1979); H. Aviv and P. Leder, *Proc. Natl. Acad. Sci. U.S.A.* **69**, 1408 (1972)] and plaques were screened with antiserum [R. Young and R. Davies, *ibid.* **80**, 1194 (1983)]. Immunoreacting plaques were purified and the insert DNA was amplified. All cDNAs isolated in this way cross-hybridized on a Southern blot and were used as probes to isolate further clones from the original cDNA library and also from a *Gga* genomic library constructed in pGM32. A 1.1-kb cDNA clone (pA312) and a 10.6-kb genomic clone (pA3G1) were selected for use in the subsequent experiment. The full DNA sequence of an additional cDNA clone (pA3171), which encompasses pA312, was determined completely for both strands (GenBank accession number U17568). This was achieved by sequencing restriction fragments of pA3171 that had been subcloned into pBluescript II SK (Stratagene, La Jolla, CA) and by use of specific primers to sequence over gaps and restriction sites. DyeDeoxy terminator cycle sequencing and the Model 373 DNA sequencing system (Applied Biosystems, La Jolla, CA) were used.

17. F. P. Buxton and A. Radford, *Mol. Gen. Genet.* **190**, 403 (1983).
18. B. Austin and B. Tyler, *Exp. Mycol.* **14**, 9 (1990).
19. D. J. Ballance and G. Turner, *Mol. Gen. Genet.* **202**, 271 (1986).
20. B. Fritig and M. Legrand, *Developments in Plant Pathology*, vol. 2 of *Mechanisms of Plant Defense Responses* (Kluwer Academic, Dordrecht, Netherlands, 1993).
21. P. Punt, R. P. Oliver, M. A. Dingemanse, P. H. Pouwels, C. A. M. J. J. van den Hondel, *Gene* **56**, 117 (1987).
22. J. M. Henson, N. K. Blake, A. L. Pilgeram, *Curr. Genet.* **14**, 113 (1988).
23. U. Raeder and P. Broda, *Lett. Appl. Microbiol.* **1**, 17 (1985).
24. Agar plugs containing the fungal inoculum were placed on 30 ml of loosely packed sterile moist vermiculite in 50-ml sterile plastic tubes and covered with a further 5 ml of wet sterile vermiculite. Mock-inoculated tubes received plugs of sterile agar. Surface-sterilized oat or wheat seeds were sown on top. A further thin layer of vermiculite was added, and the tubes were sealed with Parafilm (American National Can, Greenwich, CT). Tubes were incubated at 16°C for 20 to 25 days with a light-dark cycle of 16 hours of light to 8 hours of dark. Seedlings were carefully removed from the vermiculite 25 days after inoculation, and symptoms were scored.
25. P. Bowyer, B. R. Clarke, P. Lunness, M. J. Daniels, A. E. Osbourn, data not shown.

26. The Sainsbury Laboratory is supported by the Gatsby Charitable Foundation. This work was also supported by grants from the U.K. Agriculture and Food Research Council. We thank G. May for providing the plasmid pGM32 and M. Dow for advice on protein purification and for critically reading the manuscript.

23 August 1994; accepted 2 November 1994

Mechanisms of Rhodopsin Inactivation in Vivo as Revealed by a COOH-Terminal Truncation Mutant

Jeannie Chen,* Clint L. Makino, Neal S. Peachey, Denis A. Baylor, Melvin I. Simon

Although biochemical experiments suggest that rhodopsin and other receptors coupled to heterotrimeric guanosine triphosphate–binding proteins (G proteins) are inactivated by phosphorylation near the carboxyl (COOH)-terminus and the subsequent binding of a capping protein, little is known about the quenching process in vivo. Flash responses were recorded from rods of transgenic mice in which a fraction of the rhodopsin molecules lacked the COOH-terminal phosphorylation sites. In the single photon regime, abnormally prolonged responses, attributed to activation of individual truncated rhodopsins, occurred interspersed with normal responses. The occurrence of the prolonged responses suggests that phosphorylation is required for normal shutoff. Comparison of normal and prolonged single photon responses indicated that rhodopsin begins to be quenched before the peak of the electrical response and that quenching limits the response amplitude.

In rod photoreceptors, photoexcitation of rhodopsin triggers activation of a G protein that leads to a decrease in the intracellular concentration of guanosine 3′,5′-monophosphate (cGMP). Membrane channels gated by cGMP then close, and the rod photoreceptor hyperpolarizes (*1*). The processes mediating the recovery of the response to light are not well understood. In vitro, rhodopsin's activity can be quenched by the phosphorylation of the COOH-terminus and the subsequent binding of arrestin (*2*). It has not been demonstrated, however, that this mechanism causes shutoff in vivo. Furthermore, the kinetics of shutoff in vivo are not known.

To address these questions, we generated transgenic mice that produced a form of rhodopsin in which the COOH-terminal sites that are phosphorylated by rhodopsin kinase (*3*) or protein kinase C (*4*) were deleted (Fig. 1A). Studies on the structurally related β-adrenergic receptor indicated that removal of 15 COOH-terminal amino acids from rhodopsin would probably yield a molecule capable of excitation but resistant to shutoff (*5*). The mouse genomic construct, which contained all coding sequences and introns as well as 5 kb of the 5′ and 1.5 kb of the 3′ flanking regions, was altered by site-directed mutagenesis to create a stop codon at residue 334 (S334ter) (Fig. 1B). Expression of this transgene was restricted to rods and occurred at the same time as the expression of normal opsin during development of the retina. Because overproduction of normal or modified rhodopsin invariably causes the retina to degenerate (*6*, *7*), we screened several lines of transgenic mice for animals with low amounts of transgene expression. Four of five lines expressed high amounts of

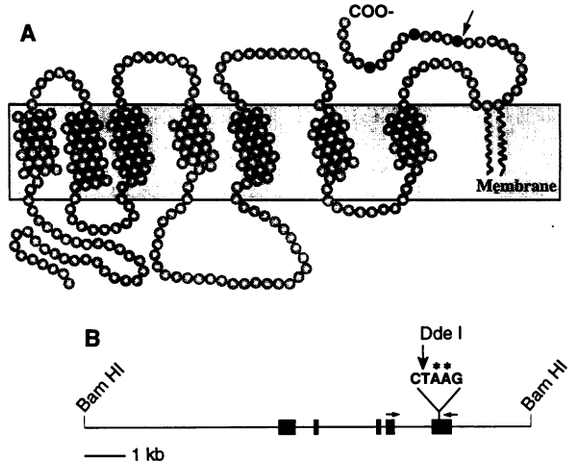

Fig. 1. Truncation mutant of rhodopsin. (**A**) A model for rhodopsin in the disc membrane (cross-sectional view, each circle representing an amino acid). Sites of rhodopsin kinase phosphorylation in normal rhodopsin are Ser^{334}, Ser^{338}, and Ser^{343} (*23*), shown by solid, filled circles. The polypeptide chain in the rhodopsin truncation mutant ended at the site marked by the arrow. (**B**) Transgene construct. The 11-kb Bam HI fragment of the mouse rhodopsin gene contained 5 kb of the 5′ upstream sequence, all coding sequences (indicated by filled boxes) and introns, and 1.5 kb of the 3′ downstream sequence. A stop codon was created at amino acid position 334 through site-specific mutagenesis of two residues (TCC → TAA; indicated by the asterisks) in exon five. This mutation also created a Dde I restriction site in the transgene construct. The arrows indicate the positions of the PCR primers used in RT-PCR (5′-GAGCTCTTCCATCTATAACCCGG-3′ and 5′-GGCTGGAGCCACCTGGCTG-3′).